OL Organic Letters

pubs.acs.org/OrgLett Letter

Evaluation of Retro-Aldol vs Retro-Carbonyl-Ene Mechanistic Pathways in a Complexity-Generating C−C Bond Fragmentation

Ana S. Bulger, Daniel W. Turner, Qingyang Zhou, K. N. Houk,* and Neil K. Garg*

Cite This: *Org. Lett.* 2024, 26, 3602−3606 Read Online

ACCESS | Metrics & More | Article Recommendations | Supporting Information

ABSTRACT: We report an experimental and computational investigation of the likely mechanism of a cascade reaction. The reaction involves an intramolecular Diels−Alder reaction, followed by a C−C bond cleavage, to afford a complex bridged bicyclic product. As multiple reaction pathways could be envisioned for the latter step, the mechanism of the C−C bond cleavage step was investigated. Two reasonable reaction pathways were evaluated. Both computations and experiments indicate that the C−C bond cleavage step proceeds by a retro-carbonyl-ene pathway rather than a retro-aldol pathway. This report underscores the synergy between computational and experimental studies and establishes the mechanism of an interesting complexity-generating transformation.

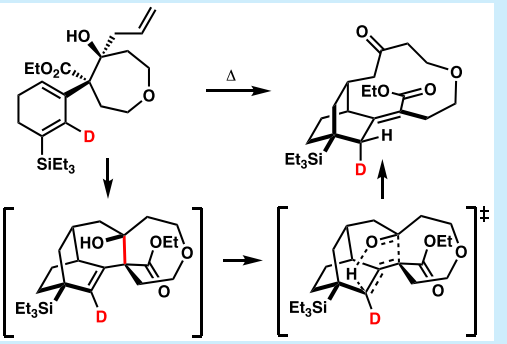

Cyclic strained intermediates that bear a functional group with a preferred linear geometry have been of great interest to the synthetic community for several decades. Such compounds, such as benzyne (**1**), indolyne **2**, and strained cyclic allene **3** (Figure 1A), have seen use in a variety of applications. This includes, but is not limited to, use of strained intermediates toward the synthesis of important molecules such as bioactive compounds,[1−7] natural products,[8−16] DNA-encoded libraries,[17] ligands,[18,19] and stimulus-responsive materials.[20] A related class of strained intermediates comprises 1,2,3-cyclohexatrienes (**4**, Figure 1B). Such intermediates and their substituted derivatives are far less studied,[21−25] but have been employed in a variety of trapping experiments. Trapping reactions of **4** lead to functionalized dienes **5** that are poised to undergo further manipulation.

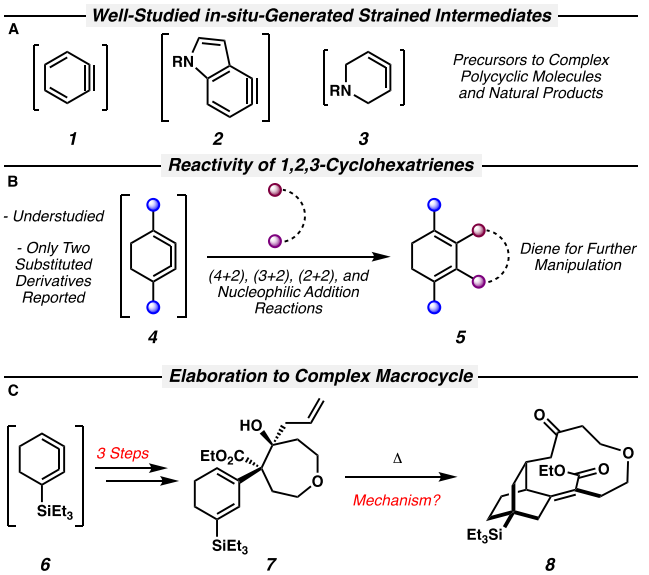

Figure 1. A) Prior studies of strained intermediates. B) Reactivity of 1,2,3-cyclohexatrienes. C) Elaboration of triene **6** to adduct **8**.

The present study pertains to the sequence summarized in Figure 1C, involving the trapping of silyl-substituted 1,2,3-cyclic triene **6** and further manipulations of its corresponding product.[25] To further explore the use of cumulated trienes as building blocks for complex scaffold synthesis, we accessed adduct **7** from intermediate **6** using a facile three-step sequence later detailed in Figure 2. Upon thermolysis of **7**, a Diels−Alder cycloaddition occurred with a subsequent rearrangement of the carbon skeleton to deliver macrocycle **8**. We describe our computational and experimental studies to interrogate the reaction mechanism for the formation of macrocycle **8**.

As shown in Figure 2, triene precursor **9** and enamine **10** are treated with fluoride-based conditions to presumably form cumulated triene **6**, which, in turn, undergoes nucleophilic trapping by enamine **10**. Subsequent acid-promoted hydrolysis yielded adduct **11**. Of note, the trapping reaction occurs regioselectively, which we have previously attributed to the presence of the bulky silyl group.[25] Subsequent addition of allyl

Received: March 22, 2024
Revised: April 12, 2024
Accepted: April 16, 2024
Published: April 22, 2024

https://doi.org/10.1021/acs.orglett.4c01037
Org. Lett. 2024, 26, 3602−3606

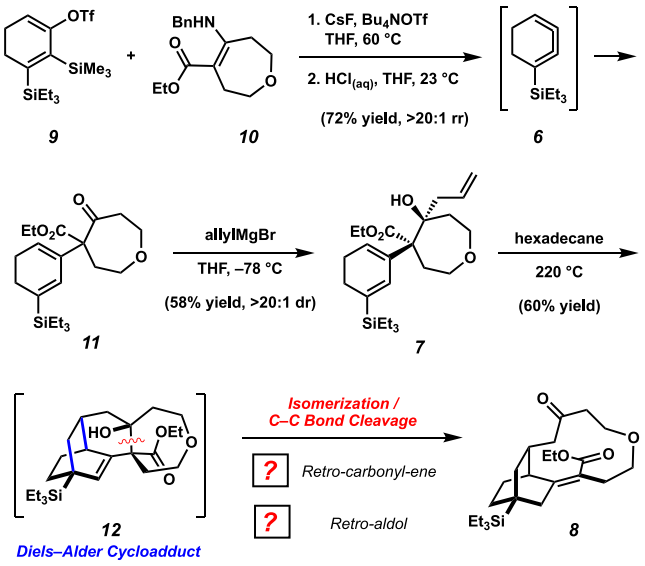

Figure 2. Trapping of 1,2,3-triene **6** and elaboration to **8** via retro-carbonyl-ene reaction or retro-aldol reaction.

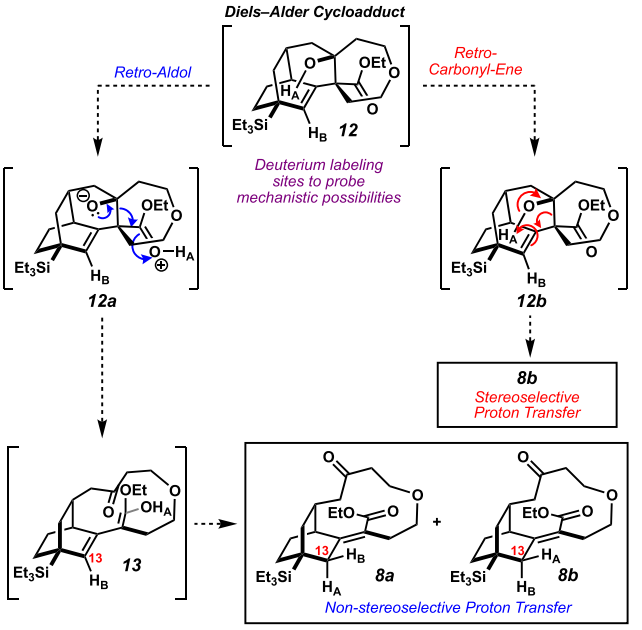

Figure 3. Details of plausible mechanistic pathways.

Grignard provided **7** via a diastereoselective 1,2-addition. In the key transformation we study herein, heating of **7** in hexadecane at 220 °C is presumed to facilitate Diels–Alder cycloaddition to give intermediate **12**. However, **12** was not observed or isolated; instead, macrocycle **8** was observed. Product **8** was thought to arise via an isomerization and C–C bond cleavage pathway, but the details of the mechanism were unknown. Two plausible pathways were deemed most viable: a retro-carbonyl-ene reaction and a retro-aldol reaction. Importantly, these two competing pathways have been the subject of both experimental and computational study for several years.[26−29] Furthermore, a better understanding of these mechanisms can inform our predictive ability and the application of such reactions[30,31] in the future construction of complex molecules, such as natural products. In this Letter, we have combined DFT calculations and experimental studies to establish the likely mechanistic pathway for the formation of macrocycle **8**.

Figure 3 depicts the two different reaction pathways (retro-aldol and retro-carbonyl-ene reactions) that can be differentiated by tracking two key hydrogen atoms (i.e., H_A and H_B) in the conversion of Diels–Alder cycloadduct **12** to macrocycle **8**. In the retro-aldol pathway, proton transfer would allow for C–C bond cleavage (see transition structure **12a**[32]) and afford enol **13**. Subsequent protonation of the extended enol on C13 could occur without appreciable stereoselectivity, leading to formation of both **8a** and **8b**.[33] Alternatively, the concerted retro-carbonyl-ene mechanism would proceed through a completely stereoselective proton transfer through transition structure **12b** to give only **8b**. Given this rationale, we envisioned that deuterium labeling the positions at either H_A or H_B in structure **12** could also allow us to assess which mechanism is likely operative.

Prior to performing the deuterium labeling experiments, the two potential mechanistic pathways were evaluated computationally using DFT (Figure 4). Calculations were performed using ωB97X-D/def2-TZVPP/SMD(*n*-hexadecane)//ωB97X-D/def2-SVP/IEEPCM(*n*-hexadecane), as this functional has performed well previously in modeling the transition structures of other pericyclic reactions.[34,35] The first barrier for intramolecular Diels–Alder cycloaddition of **7** to give cycloadduct **12** was calculated to be the highest barrier of the cascade reaction at 28.7 kcal/mol (see **TS1**). The Diels–Alder cycloaddition is thought to proceed through a concerted asynchronous mechanism, which is demonstrated by the different lengths of the forming C–C bonds shown in the computed structure of **TS1**. The barriers for the retro-aldol and retro-carbonyl-ene mechanisms were also evaluated. The retro-carbonyl-ene pathway to give **8** was calculated to proceed with an activation barrier of 22.5 kcal/mol (**TS2**). Despite attempts to find a transition state structure for the retro-aldol pathway, a transition state could not be found, even under conditions using a more polar solvent (i.e., DMSO). Thus, a base catalyst is likely required for such a transformation. Inclusion of methylamine as a base gave a transition state for the retro-aldol mechanism that is predicted to be higher in energy than the retro-carbonyl-ene pathway (see Supporting Information for more details). Therefore, these computations predict that the retro-carbonyl-ene pathway is preferred over the retro-aldol alternative reaction pathway.

With computational results in hand, we pursued deuterium-labeling experiments, as alluded to earlier. Although initial efforts aimed at labeling H_A (see **12**, Figure 3) were unsuccessful,[36] the alternative strategy of labeling H_B[37] proved fruitful (Figure 5). Silyl-substituted triene precursor **9** and labeled enamine **10**-*d* (93% deuterium incorporation) were carried through the synthetic sequence to furnish **7**-*d* (79% deuterium incorporation).[38] The first step, as previously shown in Figure 2, involves trapping of the 1,2,3-triene intermediate. Transition structure **14**-*d* suggests a plausible mechanism by which deuterium incorporation occurs in the triene trapping experiment. In the key mechanistic experiment, **7**-*d* was heated at 220 °C in hexadecane to provide the product **8**-*d*. ^{1}H NMR analysis indicated that proton transfer occurred to give exclusive C13 deuteration at the pseudoaxial position (79% deuterium incorporation). This result is consistent with transition structure **12b** (see Figure 3) and the retro-carbonyl-ene mechanism, rather than the retro-aldol pathway.

https://doi.org/10.1021/acs.orglett.4c01037
Org. Lett. 2024, 26, 3602−3606

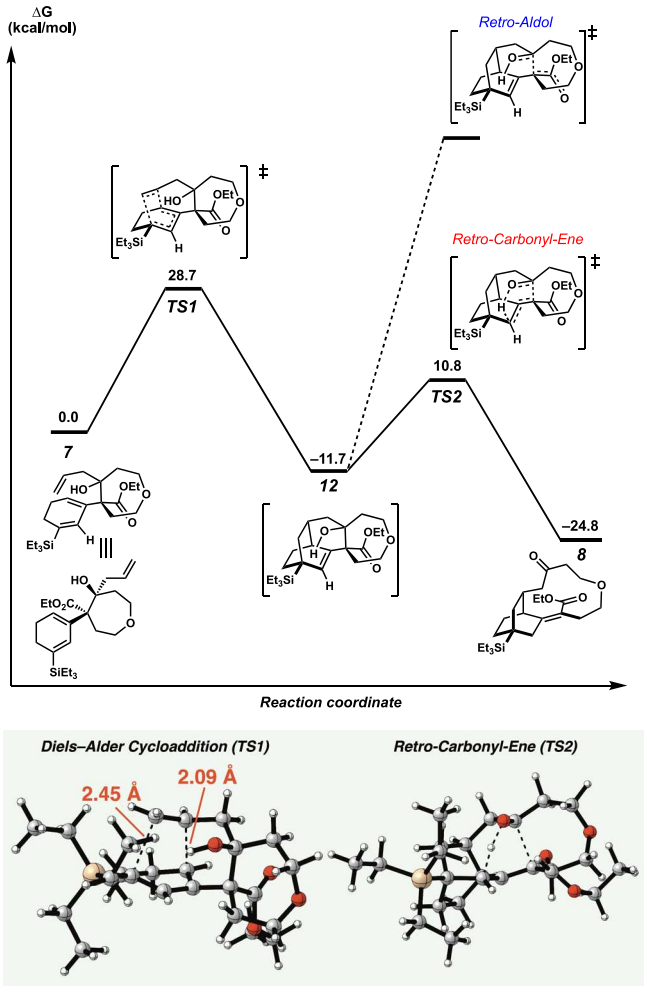

Figure 4. Computational study of reaction pathways predicts the retro-carbonyl-ene pathway is favorable. Energies were calculated using ωB97X-D/def2-TZVPP/SMD(*n*-hexadecane)//ωB97X-D/def2-SVP/IEFPCM(*n*-hexadecane) and are given in kcal/mol. Computed transition states **TS1** and **TS2** are shown.

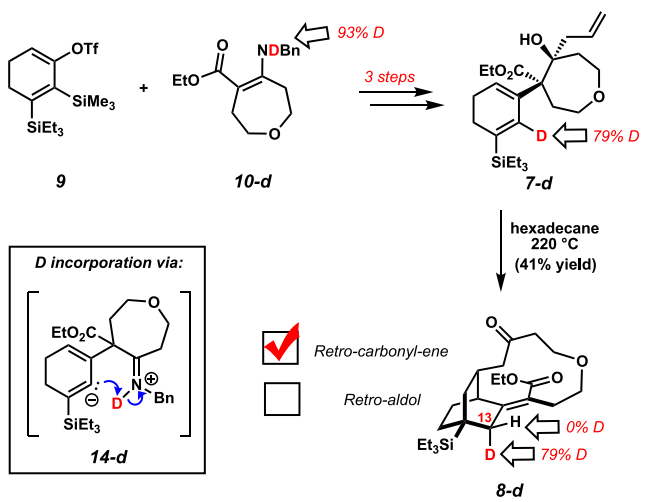

Figure 5. Synthesis of **8**-*d* and results of Diels–Alder/rearrangement cascade indicating a retro-carbonyl-ene pathway.

As such, this result is consistent with computational results described earlier.

We studied the transformation of **7** to **8** through both computational and empirical methods. Calculations predicted that a retro-carbonyl-ene reaction pathway was operative, and this hypothesis was confirmed experimentally through a deuterium labeling study. This report underscores the synergy between computational and experimental studies and establishes the mechanism of this interesting complexity-generating transformation. We hope these studies may enable the further use of the retro-carbonyl-ene reaction in total synthesis and encourage the further use of computations and experiments, in tandem, to interrogate mechanistic pathways.

■ ASSOCIATED CONTENT

Data Availability Statement

The data underlying this study are available in the published article and its Supporting Information.

Supporting Information

The Supporting Information is available free of charge at https://pubs.acs.org/doi/10.1021/acs.orglett.4c01037.

Experimental details, compound characterization data, additional computational results, Cartesian coordinates of calculated structures, and NMR spectra (PDF)

■ AUTHOR INFORMATION

Corresponding Authors

K. N. Houk − *Department of Chemistry and Biochemistry, University of California, Los Angeles, California 90095-1569, United States;* orcid.org/0000-0002-8387-5261; Email: houk@chem.ucla.edu

Neil K. Garg − *Department of Chemistry and Biochemistry, University of California, Los Angeles, California 90095-1569, United States;* orcid.org/0000-0002-7793-2629; Email: neilgarg@chem.ucla.edu

Authors

Ana S. Bulger − *Department of Chemistry and Biochemistry, University of California, Los Angeles, California 90095-1569, United States*

Daniel W. Turner − *Department of Chemistry and Biochemistry, University of California, Los Angeles, California 90095-1569, United States*

Qingyang Zhou − *Department of Chemistry and Biochemistry, University of California, Los Angeles, California 90095-1569, United States*

Complete contact information is available at: https://pubs.acs.org/10.1021/acs.orglett.4c01037

Notes

The authors declare no competing financial interest.

■ ACKNOWLEDGMENTS

The authors are grateful to the University of California, Los Angeles, NIH-NIGMS (R35 GM139593 for N.K.G), the Trueblood Family (N.K.G.), the National Science Foundation GRFP (DGE-2934835 for A.S.B.), and the Foote Family (for A.S.B.). These studies were supported by shared instrumentation grants from the NSF (CHE-1048804) and the NIH NCRR (S10RR025631). The authors acknowledge the NSF (CHE-2153972 for K.N.H.) and computational resources from Expanse at SDSC through allocation CHE040014 from the

https://doi.org/10.1021/acs.orglett.4c01037
Org. Lett. 2024, 26, 3602−3606

Advanced Cyberinfrastructure Coordination Ecosystem: Services & Support (ACCESS) program (for K.N.H. and Q.Z.). The authors also wish to acknowledge Professor Reinhard W. Hoffmann (Philipps-Universität Marburg) and Lisa Kamecke (University of Münster) for thoughtful suggestions.

REFERENCES

(1) Carroll, F. I.; Robinson, T. P.; Brieaddy, L. E.; Atkinson, R. N.; Mascarella, S. W.; Damaj, M. I.; Martin, B. R.; Navarro, H. A. Synthesis and Nicotinic Acetylcholine Receptor Binding Properties of Bridged and Fused Ring Analogues of Epibatidine. *J. Med. Chem.* **2007**, *50*, 6383−6391.
(2) Kametani, T.; Kigasawa, K.; Hiiragi, M.; Wagatsuma, N.; Uryu, T.; Araki, K. Syntheses of Heterocyclic Compounds. 509. Syntheses of Analgesics. 34. Synthesis of 3-Hydroxy-N-Cyclopropylmethyl-9-Azamorphinan. *J. Med. Chem.* **1973**, *16*, 301−303.
(3) Heindel, N. D.; Fives, W. P.; Lemke, T. F.; Rowe, J. E.; Snady, H. W.; Carrano, R. A. Synthesis, Transformation, and General Pharmacologic Activity in 1,4-Benzodiazepine-3,5-diones. *J. Med. Chem.* **1971**, *14*, 1233−1235.
(4) Bell, M. R.; Zalay, A. W.; Oesterlin, R.; Schane, P.; Potts, G. Basic Ethers of 1-(p-Hydroxyphenyl)-2-Phenyl-1,2,3,4-Tetrahydroquinoline and 1-(p-Hydroxyphenyl)-2-Phenyl Indole Antifertility Agents. *J. Med. Chem.* **1970**, *13*, 664−668.
(5) Willis, P. G.; Pavlova, O. A.; Chefer, S. I.; Vaupel, D. B.; Mukhin, A. G.; Horti, A. G. Synthesis and Structure-Activity Relationship of a Novel Series of Aminoalkylindoles with Potential of Imaging the Neuronal Cannabinoid Receptor by Positron Emission Tomography. *J. Med. Chem.* **2005**, *48*, 5813−5822.
(6) Jacob, P., III; Shulgin, A. T. Sulfur Analogues of Psychotomimetic Agents. Monothio Analogues of Mescaline and Isomescaline. *J. Med. Chem.* **1981**, *24*, 1348−1353.
(7) Coe, J. W.; Brooks, P. R.; Wirtz, M. C.; Bashore, C. G.; Bianco, K. E.; Vetelino, M. G.; Arnold, E. P.; Lebel, L. A.; Fox, C. B.; Tingley, F. D., III; Schulz, D. W.; Davis, T. I.; Sands, S. B.; Mansbach, R. S.; Rollema, H.; O'Neill, B. T. 3,5-Bicyclic Aryl Piperidines: A Novel Class of $\alpha4\beta2$ Neuronal Nicotinic Receptor Partial Agonists for Smoking Cessation. *Bioorg. Med. Chem. Lett.* **2005**, *15*, 4889−4897.
(8) Kou, K. G. M.; Pflueger, J. J.; Kiho, T.; Morrill, L. C.; Fisher, E. L.; Clagg, K.; Lebold, T. P.; Kisunzu, J. K.; Sarpong, R. A Benzyne Insertion Approach to Hetisine-Type Diterpenoid Alkaloids: Synthesis of Cossonidine (Davisine). *J. Am. Chem. Soc.* **2018**, *140*, 8105−8109.
(9) Goetz, A. E.; Silberstein, A. L.; Corsello, M. A.; Garg, N. K. Concise Enantiospecific Total Synthesis of Tubingensin A. *J. Am. Chem. Soc.* **2014**, *136*, 3036−3039.
(10) Tadross, P. M.; Stoltz, B. M. A Comprehensive History of Arynes in Natural Product Total Synthesis. *Chem. Rev.* **2012**, *112*, 3550−3577.
(11) Gampe, C. M.; Carreira, E. M. Arynes and Cyclohexyne in Natural Product Synthesis. *Angew. Chem., Int. Ed.* **2012**, *51*, 3766−3778.
(12) Corsello, M. A.; Kim, J.; Garg, N. K. Total Synthesis of (−)-Tubingensin B Enabled by the Strategic Use of an Aryne Cyclization. *Nat. Chem.* **2017**, *9*, 944−949.
(13) Gampe, C. M.; Carreira, E. M. Total Syntheses of Guanacastepenes N and O. *Angew. Chem., Int. Ed.* **2011**, *50*, 2962−2965.
(14) Nathel, N. F. F.; Shah, T. K.; Bronner, S. M.; Garg, N. K. Total Syntheses of Indolactam Alkaloids (−)-Indolactam V, (−)-Pendolmycin, (−)-Lyngbyatoxin A, and (−)-Teleocidin A-2. *Chem. Sci.* **2014**, *5*, 2184−2190.
(15) Ippoliti, F. M.; Adamson, N. J.; Wonilowicz, L. G.; Nasrallah, D. J.; Darzi, E. R.; Donaldson, J. S.; Garg, N. K. Total Synthesis of Lissodendoric Acid A via Stereospecific Trapping of a Strained Cyclic Allene. *Science* **2023**, *379*, 261−265.
(16) Mehta, M. M.; Gonzalez, J. A. M.; Bachman, J. L.; Garg, N. K. Cyclic Allene Approach to the Manzamine Alkaloid Keramaphidin B. *Org. Lett.* **2023**, *25*, 5553−5557.
(17) Westphal, M. V.; Hudson, L.; Mason, J. W.; Pradeilles, J. A.; Zécri, F. J.; Briner, K.; Schreiber, S. L. Water-Compatible Cycloadditions of Oligonucleotide-Conjugated Strained Allenes for DNA-Encoded Library Synthesis. *J. Am. Chem. Soc.* **2020**, *142*, 7776−7782.
(18) Surry, D. S.; Buchwald, S. L. Biaryl Phosphane Ligands in Palladium-Catalyzed Amination. *Angew. Chem., Int. Ed.* **2008**, *47*, 6338−6361.
(19) Mauger, C. C.; Mignani, G. A. An Efficient and Safe Procedure for the Large-Scale Pd-Catalyzed Hydrazonation of Aromatic Chlorides Using Buchwald Technology. *Org. Process Res. Dev.* **2004**, *8*, 1065−1071.
(20) Darzi, E. R.; Barber, J. S.; Garg, N. K. Cyclic Alkyne Approach to Heteroatom-Containing Polycyclic Aromatic Hydrocarbon Scaffolds. *Angew. Chem., Int. Ed.* **2019**, *58*, 9419−9424.
(21) Shakespeare, W. C.; Johnson, R. P. 1,2,3-Cyclohexatriene and Cyclohexen-3-yne: Two New Highly Strained C_6H_6 Isomers. *J. Am. Chem. Soc.* **1990**, *112*, 8578−8579.
(22) Hickey, E. R.; Paquette, L. A. Torsional Angle Decompression is not the Source of Facial Selectivity in Diels−Alder Cycloadditions Involving Cyclic Dienes Fused to Bicyclic Frameworks. The Case Study of 1,2,3,4,6,7-Hexahydro-1,4-Methanonaphthalene. *Tetrahedron Lett.* **1994**, *35*, 2309−2312.
(23) Burrell, R. C.; Daoust, K. J.; Bradley, A. Z.; DiRico, K. J.; Johnson, R. P. Strained Cyclic Cumulene Intermediates in Diels−Alder Cycloadditions of Enynes and Diynes. *J. Am. Chem. Soc.* **1996**, *118*, 4218−4219.
(24) Sakura, M.; Ando, S.; Hattori, A.; Saito, K. Reaction of Cyclohexa-1,2,3-Triene with *N*,α-Diphenylnitrone: Formation of Seven-Membered Cyclic Amines via Piradone Derivatives. *Heterocycles* **1999**, *51*, 547−556.
(25) Kelleghan, A. V.; Bulger, A. S.; Witkowski, D. C.; Garg, N. K. Strain-Promoted Reactions of 1,2,3-Cyclohexatriene and its Derivatives. *Nature* **2023**, *618*, 748−754.
(26) Ranganathan, S.; Kumar, R.; Maniktala, V. On the Mechanism and Synthetic Applications of the Thermal and Alkaline Degradation of C-18 Castor Oil. *Tetrahedron* **1984**, *40*, 1167−1168.
(27) Setzer, W. N. A DFT Analysis of Thermal Decomposition Reactions Important to Natural Products. *Nat. Prod. Commun.* **2010**, *5*, 993−998.
(28) Goussougli, M.; Sirjean, B.; Glaude, P.-A.; Fournet, R. Theoretical Study of the Pyrolysis of β-1,4-Xylan: A Detailed Investigation on Unimolecular Concerted Reactions. *Phys. Chem. Chem. Phys.* **2021**, *23*, 2605−2621.
(29) Liu, S.; Zhang, T.; Zhu, L.; Zhong, K.; Gong, J.; Yang, Z.; Bai, R.; Lan, Y. Retro-Metal-Ene Versus Retro-Aldol: Mechanistic Insight into Rh-catalysed Formal [3 + 2] Cycloaddition. *Chem. Commun.* **2018**, *54*, 13551−13554.
(30) Talanquer, V. Importance of Understanding Fundamental Chemical Mechanisms. *J. Chem. Educ* **2018**, *95*, 1905−1911.
(31) Chin, Y. P.; See, N. W.; Jenkins, I. D.; Krenske, E. H. Computational Discoveries of Reaction Mechanisms: Recent Highlights and Emerging Challenges. *Org. Biomol. Chem.* **2022**, *20*, 2028−2042.
(32) Alternatively, C−C bond cleavage could precede proton transfer.
(33) Although a mixture could be obtained, we would expect this pathway could give a preference for the formation of **8a** based on kinetic protonation of **13** on the less hindered face of the extended enol on C13.
(34) Linder, M.; Brinck, T. On the Method-Dependence of Transition State Asynchronicity in Diels−Alder Reactions. *Phys. Chem. Chem. Phys.* **2013**, *15*, 5108−5114.
(35) Goerigk, L.; Hansen, A.; Bauer, C.; Ehrlich, S.; Najibi, A.; Grimme, S. A Look at the Density Functional Theory Zoo with the Advanced GMTKN55 Database for General Main Group Thermo-

https://doi.org/10.1021/acs.orglett.4c01037
Org. Lett. 2024, 26, 3602−3606

chemistry, Kinetics and Noncovalent Interactions. *Phys. Chem. Chem. Phys.* **2017**, *19*, 32184−32215.
(36) H/D exchange of the hindered tertiary alcohol was found to be challenging.
(37) Picazo, E.; Anthony, S. M.; Giroud, M.; Simon, A.; Miller, M. A.; Houk, K. N.; Garg, N. K. Arynes and Cyclic Alkynes as Synthetic Building Blocks for Stereodefined Quaternary Centers. *J. Am. Chem. Soc.* **2018**, *140*, 7605−7610.
(38) Deuterium incorporation was determined by ^{1}H NMR analysis. Relative integration of the signal corresponding to the labeled atom informed the extent of hydrogen retention and deuterium incorporation. Deuterium presence was confirmed by ^{2}H NMR analysis and HRMS.

https://doi.org/10.1021/acs.orglett.4c01037
Org. Lett. 2024, 26, 3602−3606